

## Supplementary Materials for

### Extracellular $\text{Ca}^{2+}$ Acts as a Mediator of Communication from Neurons to Glia

Arnulfo Torres, Fushun Wang, Qiwu Xu, Takumi Fujita, Radoslaw Dobrowolski, Klaus Willecke, Takahiro Takano, Maiken Nedergaard\*

\*To whom correspondence should be addressed. E-mail: nedergaard@urmc.rochester.edu

Published 24 January 2012, *Sci. Signal.* **5**, ra8 (2012)  
DOI: 10.1126/scisignal.2002160

#### The PDF file includes:

- Fig. S1. Calibration of  $\text{Ca}^{2+}$ -sensitive microelectrode and effects of diazo-2 photolysis on  $[\text{Ca}^{2+}]_e$ .
- Fig. S2. CA1 pyramidal neurons depolarize and decrease their input resistance in response to photolysis of MNI-glutamate, whereas photolysis of diazo-2 is not associated with changes in the membrane properties.
- Fig. S3. Photolysis of MNI-glutamate.
- Fig. S4. Transgenic reporter mice reveal distinct responses to MNI-glutamate photolysis of neurons and astrocytes in hippocampal slices.
- Fig. S5. Comparison of  $\text{Ca}^{2+}$  waves in hippocampus and cortex evoked by photolysis of MNI-glutamate and diazo-2.
- Fig. S6. Comparison of  $\text{Ca}^{2+}$  waves evoked by diazo-2 and MNI-glutamate photolysis.
- Fig. S7. Effect of manipulation of P2Y1 receptors in hippocampal interneurons.

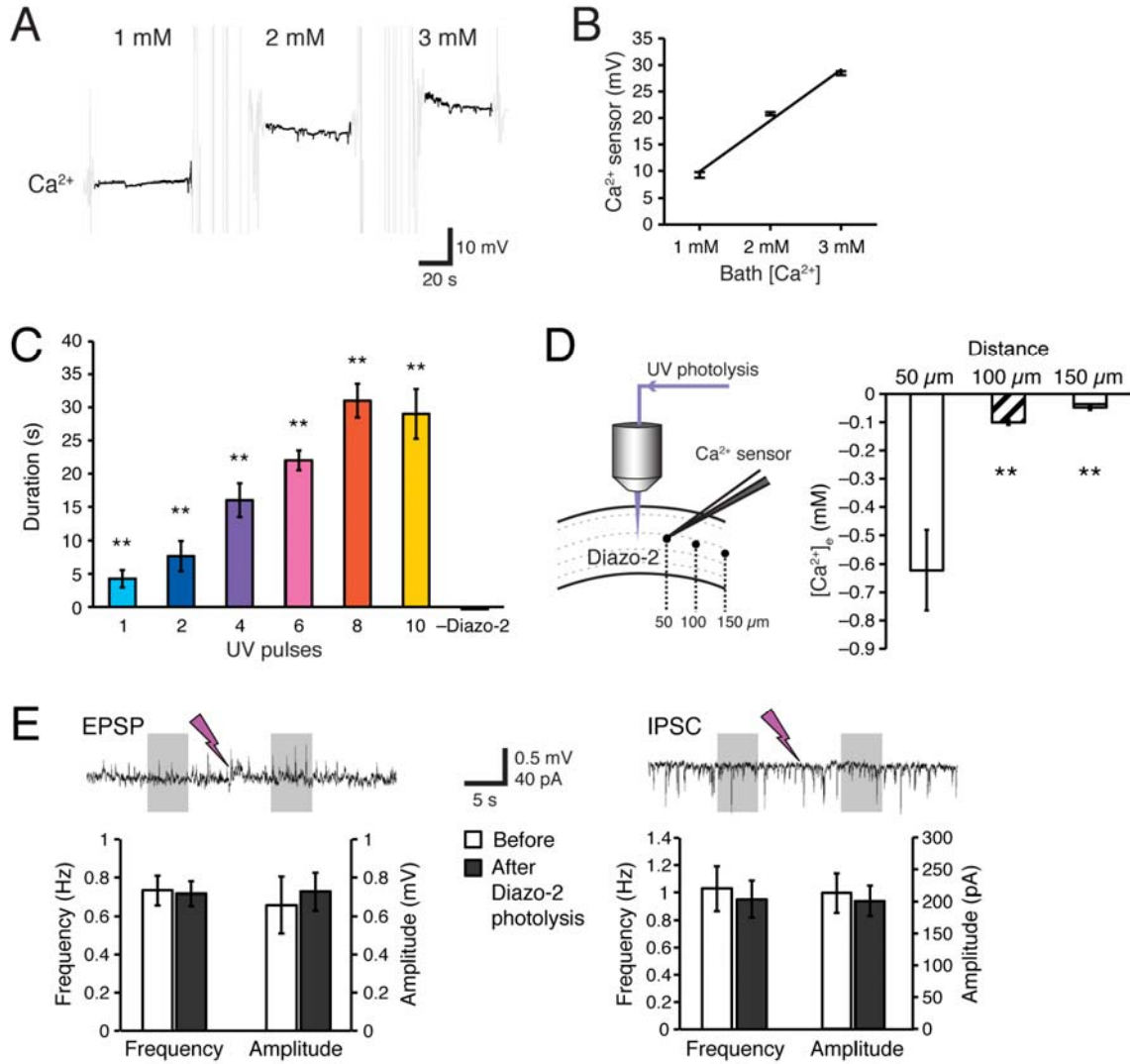


**Fig. S1. Calibration of  $\text{Ca}^{2+}$ -sensitive microelectrode and effects of diazo-2 photolysis on  $[\text{Ca}^{2+}]_e$**

(A) Representative trace of calibration of a  $\text{Ca}^{2+}$ -sensitive microelectrode. Extracellular  $\text{Ca}^{2+}$  in the bath was successively increased from 1, to 2, to 3 mM  $\text{Ca}^{2+}$  in aCSF. (B) Calibration of  $\text{Ca}^{2+}$  sensitive microelectrodes in aCSF ( $n=3$  microelectrodes,  $r^2=0.986$ ). The electrodes used in experiments typically showed voltage responses of 5-10 mV per mM increase in  $\text{Ca}^{2+}$  concentration in the concentration range studied. Electrode calibration was done before and after each experiment. (C) Duration of diazo-2-induced decrease in  $[\text{Ca}^{2+}]_e$  plotted as a function of stimulus intensity ( $n=3$  photolysis events, UV pulses 1-10, and 10 pulses without diazo-2, \*\*,  $p<0.01$ ). (D) Diagram showing recordings obtained by placing the electrode at increasing distances from the photolysis site. Diazo-

2-induced reduction in  $[Ca^{2+}]_e$  detected with the  $Ca^{2+}$ -sensitive microelectrode placed 50, 100, or 150  $\mu m$  from the site targeted by photolysis. (n=8 photolysis events, \*\*,  $p < 0.01$  compared to 50  $\mu m$ ). (E) Traces show representative recordings of spontaneous EPSPs and IPSCs in hippocampal CA1 neurons. Bar histograms compare the frequency and amplitude of EPSPs and IPSCs 5 s before or 5 s after photolysis (no significant differences in EPSP or IPSC frequency and amplitude was identified using paired t-test, before vs. after,  $p > 0.05$ , n = 7).

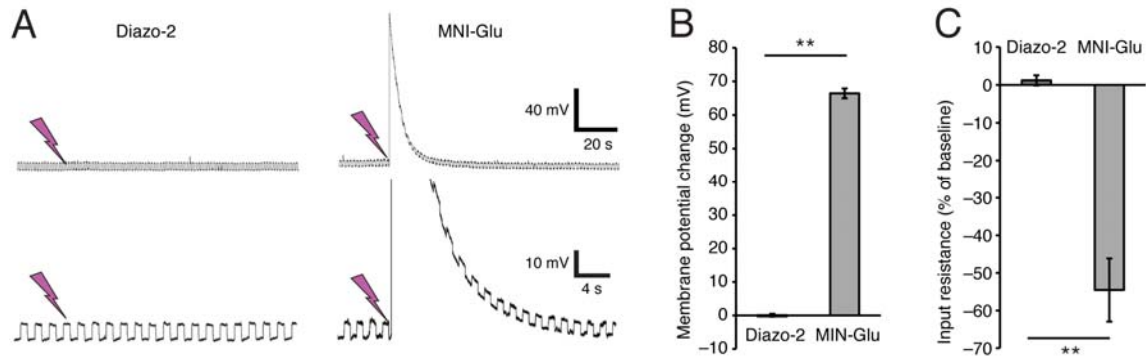


**Fig. S2. CA1 pyramidal neurons depolarize and decrease their input resistance in response to photolysis of MNI-glutamate, whereas photolysis of diazo-2 is not associated with changes in the membrane properties**

(A) Representative current-clamp recordings from a hippocampal CA1 pyramidal cell located  $\sim 70 \mu\text{m}$  from the site of photolysis of diazo-2 (left panel) or MNI-glutamate (right panel). Lower traces show expanded timescale. (B) Comparison of changes in plasma membrane potential in response to photolysis of diazo-2 and MNI-glutamate in CA1 pyramidal neurons ( $n=4-11$  photolysis events, \*\*,  $p<0.001$ ). (C) Comparison of relative changes in input resistance in response to photolysis of diazo-2 and MNI-glutamate in CA1 pyramidal neurons ( $n=4-5$  photolysis events, \*\*,  $p<0.001$ ).

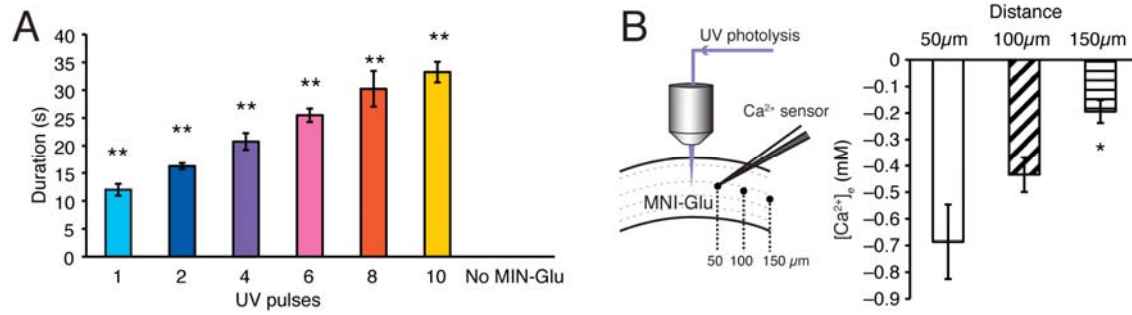


**Fig. S3. Photolysis of MNI-glutamate**

**(A)** Duration of the decrease in  $[Ca^{2+}]_e$  produced by photolysis of MNI-glutamate plotted as a function of number of UV pulses used for photolysis ( $n=5$  photolysis events, \*\*,  $p<0.01$ ). **(B)** Diagram of recordings obtained by placing the electrode at increasing distances from the photolysis site. MNI-glutamate-induced reduction in  $[Ca^{2+}]_e$  detected with the  $Ca^{2+}$ -sensitive microelectrode placed 50, 100, or 150  $\mu m$  from the site targeted by photolysis ( $n=4-15$  photolysis events. \*,  $p<0.05$  compared to 50  $\mu m$ ). If MNI-glutamate was omitted, UV pulses failed to decrease  $[Ca^{2+}]_e$ .

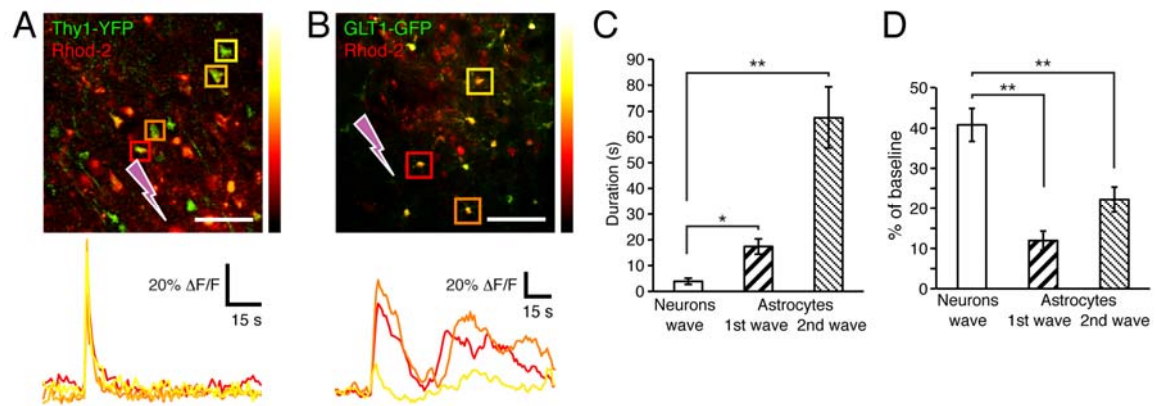


**Fig. S4. Transgenic reporter mice reveal distinct responses to MNI-glutamate photolysis of neurons and astrocytes in hippocampal slices**

(A) Hippocampal slice from a Thy1-YFP reporter mouse loaded with the Ca<sup>2+</sup> indicator rhod-2 am. YFP+ neurons show an increase in Ca<sup>2+</sup> during the 1<sup>st</sup>, but not the 2<sup>nd</sup> Ca<sup>2+</sup> wave. Scale bar, 50 μm. (B) Hippocampal slice from a GLT1-GFP reporter mouse loaded with the Ca<sup>2+</sup> indicator rhod-2 am. GFP+ astrocytes show an increase in Ca<sup>2+</sup> during both the 1<sup>st</sup> and the 2<sup>nd</sup> Ca<sup>2+</sup> waves. Scale bar, 50 μm. (C) Duration of the increase in Ca<sup>2+</sup> in astrocytes and neurons during the 1<sup>st</sup> and the 2<sup>nd</sup> Ca<sup>2+</sup> wave (n=12-13 photolysis events, \*, p<0.05, \*\*, p<0.01). (D) The amplitude of the increases in Ca<sup>2+</sup> in astrocytes or neurons during the 1<sup>st</sup> or the 2<sup>nd</sup> Ca<sup>2+</sup> wave (n=10 photolysis events, \*\*, p<0.01).

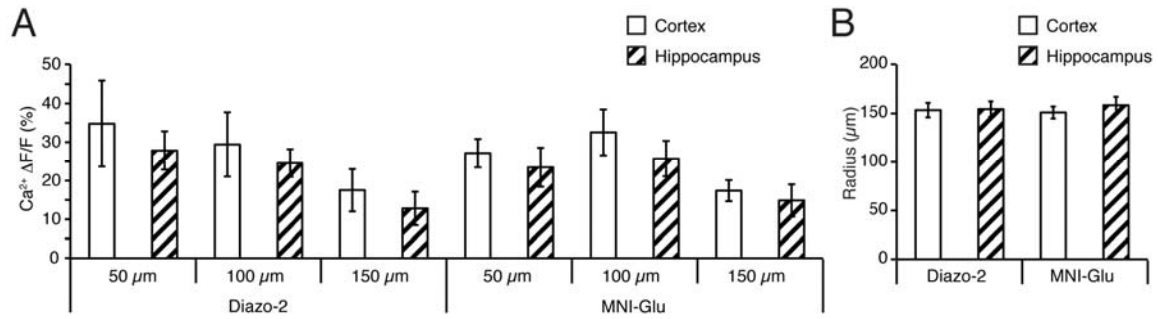


**Fig. S5. Comparison of Ca<sup>2+</sup> waves in hippocampus and cortex evoked by photolysis of MNI-glutamate or diazo-2**

(A) Comparison of Ca<sup>2+</sup> increases in astrocytes during the 2<sup>nd</sup> Ca<sup>2+</sup> wave evoked by photolysis of MNI-glutamate and the Ca<sup>2+</sup> wave evoked by photolysis of diazo-2 at 50, 100, and 150 μm in cortex and hippocampus (n=9 photolysis events, p>0.05). (B) Comparison of maximal radius of the Ca<sup>2+</sup> waves in astrocytes evoked by photolysis of MNI-glutamate and diazo-2 in cortex and hippocampus (n=10 photolysis events, p>0.05).

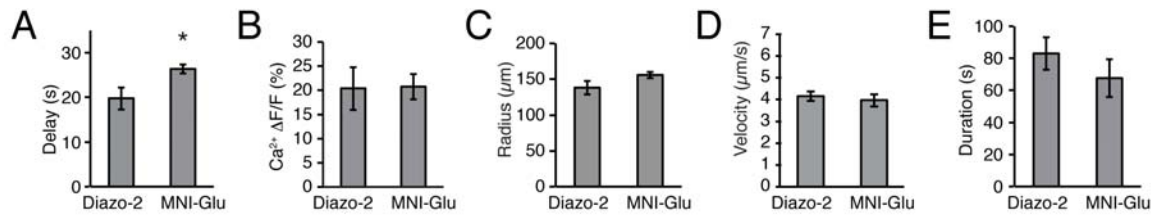


**Fig. S6. Comparison of Ca<sup>2+</sup> waves evoked by diazo-2 or MNI-glutamate photolysis**

All comparisons are made between Ca<sup>2+</sup> waves evoked by diazo-2 photolysis and the 2<sup>nd</sup> Ca<sup>2+</sup> wave evoked by MNI-glutamate. **(A)** Histogram comparing the delay between photolysis and the first increase in Ca<sup>2+</sup> evoked by diazo-2 or MNI-glutamate photolysis (n=20-22 photolysis events, \*, p<0.05). **(B)** Ca<sup>2+</sup> increase at 75 μm evoked by diazo-2 or MNI-glutamate photolysis (n=16 photolysis events). **(C)** Radius of Ca<sup>2+</sup> waves evoked by diazo-2 or MNI-glutamate photolysis (n=26 photolysis events). **(D)** Velocity of Ca<sup>2+</sup> waves evoked by diazo-2 or MNI-glutamate photolysis (n=18 photolysis events). **(E)** Duration of Ca<sup>2+</sup> increases in astrocytes evoked by diazo-2 or MNI-glutamate photolysis (n=12 photolysis events).

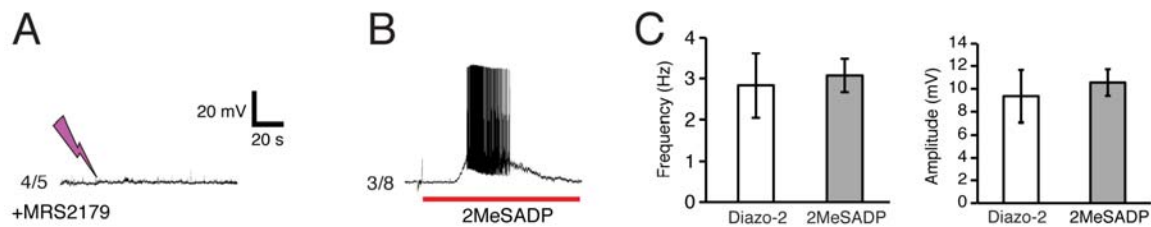


**Fig. S7. Effect of manipulation of P2Y1 receptors in hippocampal interneurons**

(A) The P2Y1 receptor antagonist, MRS2179 (50  $\mu$ M) blocked depolarization and bursting activity induced by diazo-2 photolysis in 4 of 5 interneurons. One of the five interneurons exhibited a transient minor depolarization, but no action potential firing. (B) Exposure to the P2Y1 receptor agonist 2MeSADP (100  $\mu$ M) induced depolarization in a total of 8 interneurons tested, whereof 3 exhibited bursting activity. (C) Histograms compare the frequency of interneuronal action potential firing, as well as the amplitude of membrane depolarization induced by photolysis of diazo-2 with or without exposure to 2MeSADP (n = 6-8 photolysis events).